Vibrational Energy Relaxation Rates of H_2 and D_2 in Liquid Argon via the Linearized Semiclassical Method

Irina Navrotskaya and Eitan Geva*

Department of Chemistry, University of Michigan, Ann Arbor, Michigan 48109-1055

Received: September 23, 2006; In Final Form: November 10, 2006

The vibrational energy relaxation (VER) rates for H_2 and D_2 in liquid argon ($T = 152$ K, $\rho = 1.45 \times 10^{22}$ cm^{-3}) are calculated using the linearized semiclassical (LSC) method (*J. Phys. Chem.* **2003**, *107*, 9059, 9070). The calculation is based on Fermi's golden rule. The VER rate constant is expressed in terms of the quantum-mechanical force−force correlation function, which is then estimated using the LSC method. A local harmonic approximation (LHA) is employed in order to compute the multidimensional Wigner integrals underlying the LSC approximation. The H_2−Ar and D_2−Ar interactions are described by the three-body potential of Bissonette et al. (*J. Phys. Chem. A* **1996**, *105*, 2639). The LHA-LSC-based VER rate constants for both D_2 and H_2 are found to be about 2−3 orders of magnitude slower than those obtained experimentally. However, their ratio agrees quantitatively with the corresponding experimental result. In contrast, the classical VER rate constants are found to be 8−9 orders of magnitude slower than those obtained experimentally, and their ratio is found to be qualitatively different from the corresponding experimental result.

I. Introduction

Vibrational energy relaxation (VER) is the process by which an excited vibrational mode equilibrates by transferring its excess energy into other intramolecular and/or intermolecular degrees of freedom (DOF). VER is prevalent in many systems of fundamental technological and biological importance and plays a central role in determining chemical reactivity. It is therefore not surprising that the measurement and calculation of VER rates have received much attention over the last few decades.[1−49] Recent theoretical and computational studies of VER have been mostly based on the Landau−Teller formula,[15,50,51] which gives the VER rate constant in terms of the Fourier transform (FT), at the vibrational frequency of the quantum-mechanical autocorrelation function of the fluctuating force exerted on the relaxing mode by the other DOF. In many cases, replacing the quantum-mechanical force autocorrelation function by its classical counterpart is unjustified because the frequency of the relaxing vibrational mode is either comparable to or larger than $k_B T/\hbar$. Indeed, discrepancies by many orders of magnitude have been reported between experimentally measured VER rates and those calculated using classical molecular dynamics (MD) simulations. Unfortunately, the exact calculation of real-time quantum-mechanical correlation functions for general anharmonic many-body systems remains far beyond the reach of currently available computer resources.[52] The most popular approach for dealing with this difficulty, in the case of VER, is based on multiplying the classical VER rate constant by a frequency-dependent quantum correction factor (QCF).[7,53−68] A variety of different approximate QCFs have been proposed in the literature. Unfortunately, estimates obtained from different QCFs can differ by orders of magnitude, and particularly so when high-frequency vibrations are involved. Thus, the development of more rigorous methods for computing VER rate constants is highly desirable.

In a series of recent papers,[69−72] we have proposed a more rigorous approach for calculating VER rate constants, which is based on linearizing the forward−backward action in the path-integral expression for the quantum force autocorrelation function (the linearization is with respect to the difference between the forward and backward paths[73]). It should be noted that the same approximation can be derived in several other ways, including linearization of the forward−backward action in the semiclassical initial value representation approximation for the correlation function[74−80] and starting from the Wigner representation formalism.[81] The *resulting linearized semiclassical (LSC) approximation* for a general real-time quantum mechanical correlation function is given by

$$Tr(e^{-\beta H} e^{iHt/\hbar} B e^{-iHt/\hbar} A) \approx \frac{1}{(2\pi\hbar)^N} \int \mathbf{dq}_0 \int \mathbf{dp}_0 \, (Ae^{-\beta H})_W(\mathbf{q}_0, \mathbf{p}_0) B_W(\mathbf{q}_t^{(\mathrm{Cl})}, \mathbf{p}_t^{(\mathrm{Cl})}) \quad (1)$$

where N is the number of DOF, $\mathbf{q}_0 = (q_0^{(1)}, ..., q_0^{(N)})$ and $\mathbf{p}_0 = (p_0^{(1)}, ..., p_0^{(N)})$ are the corresponding coordinates and momenta,

$$A_W(\mathbf{q}, \mathbf{p}) = \int \mathbf{d}\Delta \, e^{-i\mathbf{p}\Delta/\hbar} \langle \mathbf{q} + \Delta/2 | A | \mathbf{q} - \Delta/2 \rangle \quad (2)$$

is the Wigner transform of the operator A,[82] and $\mathbf{q}_t^{(\mathrm{Cl})} = \mathbf{q}_t^{(\mathrm{Cl})}(\mathbf{q}_0, \mathbf{p}_0)$ and $\mathbf{p}_t^{(\mathrm{Cl})} = \mathbf{p}_t^{(\mathrm{Cl})}(\mathbf{q}_0, \mathbf{p}_0)$ are propagated classically with the initial conditions $\mathbf{q}_0$ and $\mathbf{p}_0$.

The major advantage of the LSC approximation is its computational feasibility (although computing the Wigner transform in systems with many DOF is not trivial[69,70,75]). The LSC approximation has the additional attractive features of being exact at $t = 0$, at the classical limit, and for harmonic systems. Its main disadvantage is the fact that it can only capture quantum effects at short times.[76] However, it should be noted that, in condensed phase systems in general, and in the case of high-frequency VER in particular, the quantities of interest are often dominated by the short-time dynamics of the correlation functions.

* Corresponding author. E-mail: eitan@umich.edu.

10.1021/jp066243g CCC: $37.00
Published on Web 12/30/2006

In practice, using the LSC approximation, eq 1, requires the calculation of the phase-space integrals underlying the Wigner transforms. The numerical calculation of those integrals is extremely difficult in the case of many-body anharmonic systems because of the oscillatory phase factor, $e^{-i\mathbf{p}_0\Delta/\hbar}$, in the integrand. In refs 69,70, this problem was dealt with by using a local harmonic approximation (LHA), which allows for an analytical evaluation of the Wigner integral. The emerging LHA-LSC approximation has been tested on several benchmark problems in ref 69 and was found to give very good agreement with the exact results, or their best estimates. It was also observed that high-frequency VER is dominated by a purely quantum mechanical term, which is not accounted for in classical MD simulations. The first application of the LHA-LSC method to a molecular liquid was reported in ref 70, where it was used to calculate the VER rate constant in neat liquid oxygen at 77K. The VER rate constant obtained via the LHA-LSC approximation was found to be 4 orders of magnitude larger than the corresponding classical rate constant and in very good quantitative agreement with experiment. Quantitative agreement between the predictions of the LHA-LSC method and the corresponding experimental VER rates was also found for neat liquid nitrogen and oxygen−argon mixtures over a wide range of temperatures and mole fractions.[71] The range of applicability of the LHA-LSC method has also been recently extended to polyatomic molecules in liquid solution.[72]

In this paper, we use the LHA-LSC method in order to compute the VER rates of H_2 and D_2 in liquid argon. The main motivation for considering this system has to do with the fact that H_2 and D_2 are expected to give rise to very pronounced quantum effects due to their high vibrational frequencies and light masses. It should also be noted that experimental values of the VER rates in dilute H_2−Ar and D_2−Ar solutions are available over a wide range of H_2 and D_2 mole fractions.[4,19] The values of the VER rate constants at infinite dilution, which can be compared with our results, may be obtained by extrapolating the experimental results to zero H_2 and D_2 mole fractions. VER rates in this system also exhibit a rather large isotope effect. More specifically, the experimental VER rate of H_2 is an order of magnitude larger than that of D_2 under the same conditions, despite the fact that the vibrational frequency of H_2 is larger than that of D_2 by a factor of $\sqrt{2}$. The VER rates of H_2 and D_2 in liquid argon have also been recently calculated by Miller and Adelman.[83] However, the latter study was based on a classical treatment (relying on either classical MD simulations or a classical integral equation formalism) and employed a Gaussian ansatz for the force autocorrelation function. The validity of the classical treatment in this context is questionable due to the high frequencies and light masses of H_2 and D_2, and the Gaussian ansatz is inconsistent with the fact that the frequency dependence of the VER rate in nonpolar liquids is often observed to follow an exponential gap law. It should also be noted that Miller and Adelman were only able to obtain agreement with experiment by considerably changing the repulsive part of the H−Ar and D−Ar pairwise interaction potentials and that they were not able to account for the experimentally observed isotope effect. In contract, the current study is based on a semiclassical treatment, whose accuracy has been previously demonstrated in the case of heavy high-frequency diatomic molecules such as O_2 and N_2. Our analysis is also based on the assumption that the frequency dependence of the VER rate constant follows an exponential gap law, which is consistent with the data obtained from both classical and nonclassical simulations. Finally, we describe the H_2−Ar and D_2−Ar interactions by an accurate state-of-the-art three-body potential.[84]

The structure of the remainder of this paper is as follows. The model and VER theory employed are outlined in Section II. The simulation procedures are described in Section III. The simulation results are presented in Section IV and discussed in Section V. Explicit expressions for the bath Hamiltonian and the force exerted on the relaxing vibrational mode are provided in the appendix.

II. Model and Vibrational Energy Relaxation Theory

We consider a single H_2 or D_2 molecule in liquid argon. The overall Hamiltonian is given by

$$H_{\mathrm{tot}}(q) = H_{\mathrm{s}}(q) + K + U(q) \tag{3}$$

The vibrational Hamiltonian, $H_{\mathrm{s}}(q)$, is given by

$$H_{\mathrm{s}}(q) = \frac{p^2}{2\mu} + \frac{1}{2}\mu\omega_0{}^2 q^2 \tag{4}$$

where q is the vibrational coordinate (i.e., the deviation of the bond length relative to its equilibrium value), p is the corresponding conjugate momentum, μ is the reduced mass, and ω_0 is the vibrational frequency. It should be noted that anharmonicity will undoubtedly become important for describing VER of highly excited states. However, in this paper we focus on VER between the first excited and ground vibrational states, for which the harmonic approximation is an excellent one.

The total rotational and translational kinetic energy, K, is given by

$$K = \frac{P_0{}^2}{2M} + \frac{L_0{}^2}{2I} + \sum_{j=1}^{N}\frac{P_j{}^2}{2m} \tag{5}$$

where m is the atomic mass of argon, M is the molecular mass of H_2 or D_2, $\mathbf{P}_j$ is the momentum of the jth argon atom, $\mathbf{P}_0$ is the molecular center of mass momentum, $\mathbf{L}_0$ is the molecular angular momentum, $I = \mu r_e^2$ is the molecular moment of inertia, and r_e is the equilibrium bond length. We have verified, via classical MD simulations, that centrifugal forces do not contribute significantly to the high-frequency VER rate in this system, which is why I is assumed to be independent of q. Finally, $U(q)$ is the overall potential energy, which is given by

$$U(q) = \sum_{j=1}^{N-1}\sum_{k=j+1}^{N}\phi_{\mathrm{Ar-Ar}}(r_{jk}) + \sum_{j=1}^{N}\phi_{\mathrm{H_2}} - \mathrm{Ar}(r_{j0},\theta_j,\mathbf{q}) \tag{6}$$

Here, $\phi_{\mathrm{Ar-Ar}}(r)$ and $\phi_{\mathrm{H_2-Ar}}(r,\theta,q)$ are the Ar−Ar and H_2−Ar interaction potentials, r_{jk} is the distance between the jth and kth argon atoms, r_{j0} is the distance between the jth argon atom and the molecular center of mass, and θ_j is the angle between the molecular axis and the vector pointing from the molecular center of mass to the jth argon atom ($0 \le \theta_j \le \pi/2$).

The Ar−Ar interaction potential is assumed to be of the Lennard-Jones type,

$$\phi_{\mathrm{Ar-Ar}}(r) = 4\epsilon\left[\left(\frac{\sigma}{r}\right)^{12} - \left(\frac{\sigma}{r}\right)^{6}\right] \tag{7}$$

with $\epsilon/k_{\mathrm{B}} = 119.8$ K and $\sigma = 3.405$ Å.[85] The interaction between the jth argon atom and the H_2 molecule is described by the three-body potential of Bissonette et al.[84] The latter is based on an

exchange-Coulomb potential model with five parameters that were determined empirically by fitting to an extensive set of spectroscopic, scattering, and thermodynamic data. More explicitly

$$\phi_{H_2-Ar}(R,\theta,q) = V_{HL}(R,\theta,q) + V_C(R,\theta,q) \quad (8)$$

where $V_{HL}(R,\theta,q)$ corresponds to the mostly repulsive short-range Heitler−London interactions, and $V_C(R,\theta,q)$ corresponds to attractive long-range multipolar interactions. Explicit expressions for these potential functions and the values of the parameters used in them can be found in ref 84.

The force $F = -[\partial U(q)/\partial q]_{q=0}$ exerted on the vibrational coordinate by the other DOF is obtained by expanding $U(q)$ to first order with respect to q:

$$U(q) \simeq U(q=0) - q\left[-\frac{\partial U(q)}{\partial q}\right]_{q=0} = U(0) - qF \quad (9)$$

Thus, the overall Hamiltonian, eq 3, can now be put in the following system-bath form,

$$H_{tot}(q) = H_s(q) + H_b - qF \quad (10)$$

where $H_b = K + U(0)$ is the bath Hamiltonian. More explicit expressions for $U(0)$ and F are provided in the appendix.

The relaxation rate constant from the first excited vibrational state of the H_2 or D_2 molecule to its ground state is given by the Landau−Teller formula:[15,50]

$$k_{0\to 1} = \frac{1}{2\mu\hbar\omega_0}\tilde{C}(\omega_0) \quad (11)$$

where

$$\tilde{C}(\omega) = \int_{-\infty}^{\infty} dt e^{i\omega t} C(t) = \frac{4}{1+e^{-\beta\hbar\omega}}\int_0^{\infty} dt \cos(\omega t) C_R(t)$$
$$= -\frac{4}{1-e^{-\beta\hbar\omega}}\int_0^{\infty} dt \sin(\omega t) C_I(t) \quad (12)$$

and

$$C(t) = C_R(t) + iC_I(t) = \langle \delta F(t)\delta F\rangle_b = \frac{1}{Z_b} Tr[e^{-\beta H_b} e^{iH_b t/\hbar}\delta F e^{-iH_b t/\hbar}\delta F] \quad (13)$$

Here, $C_R(t)$ and $C_I(t)$ are the real and imaginary parts of the force−force correlation function (FFCF), $C(t)$, respectively, $\langle A\rangle_b = Tr[e^{-\beta H_b}A]/Z_b$, $\beta = 1/k_B T$, $Z_b = Tr[e^{-\beta H_b}]$, and $\delta F = F - \langle F\rangle_b$. Equation 11 gives the VER rate constant, $k_{0\leftarrow 1}$, in terms of the FT, at the vibrational frequency, ω_0, of the FFCF, $C(t)$. We also note that in the classical limit, $k_{0\leftarrow 1}$ is given by

$$k_{0\leftarrow 1}^{cl} = \frac{1}{2\mu\hbar\omega_0}\tilde{C}_{cl}(\omega_0) \quad (14)$$

where $\tilde{C}_{cl}(\omega_0)$ is the FT of the *classical* FFCF:

$$C_{cl}(t) = \int d\mathbf{Q}_0 \int d\mathbf{P}_0 \frac{e^{-\beta H_b(\mathbf{Q}_0,\mathbf{P}_0)}}{Z_b^{cl}}\delta F(\mathbf{Q}_0)\delta F(\mathbf{Q}_t^{(cl)}) \quad (15)$$

Here, $\mathbf{Q}_t^{(cl)}$ correspond to the Cartesian coordinates and momenta of all the atoms (including those that constitute the diatomic molecule), which are propagated classically with the initial conditions $\mathbf{Q}_0$ and $\mathbf{P}_0$.

The LSC approximation of the quantum-mechanical FFCF, eq 13, has the following form:[69,70,73]

$$C(t) \approx \frac{1}{Z_b}\frac{1}{(2\pi\hbar)^f}\int d\mathbf{Q}_0 \int d\mathbf{P}_0 [\delta F e^{-\beta H_b}]_W(\mathbf{Q}_0,\mathbf{P}_0)[\delta F]_W (\mathbf{Q}_t^{(Cl)},\mathbf{P}_t^{(Cl)}) \quad (16)$$

where f is the overall number of bath DOF, and $A_W(\mathbf{Q},\mathbf{P})$ is defined as in eq 2.

The LHA is employed in order to calculate the Wigner transform $[\delta F e^{-\beta H_b}]_W(\mathbf{Q}_0,\mathbf{P}_0)$ in eq 16.[69−71] More specifically, we effectively expand H_b and F to second order around $\mathbf{Q}_0$, followed by an analytical integration over Δ of the Gaussian integral associated with $[\delta F e^{-\beta H_b}]_W(\mathbf{Q}_0,\mathbf{P}_0)/\langle \mathbf{Q}_0|e^{-\beta H_b}|\mathbf{Q}_0\rangle$. This leads to the following LHA-LSC approximation for $C(t)$:

$$C(t) \approx \int d\mathbf{Q}_0 \frac{\langle \mathbf{Q}_0|e^{-\beta H_b}|\mathbf{Q}_0\rangle}{Z_b}\int d\mathbf{P}_{n,0}\prod_{j=1}^{f}\left(\frac{1}{\alpha^{(j)}\pi\hbar^2}\right)^{1/2} \exp\left[-\frac{(P_{n,0}^{(j)})^2}{\hbar^2\alpha^{(j)}}\right][\delta F(\mathbf{Q}_0) + D(\mathbf{Q}_0,\mathbf{P}_{n,0})]\delta F(\mathbf{Q}_t^{(Cl)}) \quad (17)$$

Here, $\{P_n^{(k)}\}$ are mass-weighted normal mode momenta, as obtained from the expansion of H_b to second order around $\mathbf{Q}_0$ (the LHA), and $\alpha^{(j)} = \Omega^{(j)}\coth[\beta\hbar\Omega^{(j)}/2]/\hbar$, where $\{(\Omega^{(k)})^2\}$ are the eigenvalues of the corresponding Hessian matrix. The term $D(\mathbf{Q}_0,\mathbf{P}_{n,0})$ captures the effect of quantum nonlocality and is purely quantum-mechanical, as it vanishes at the classical ($\hbar\to 0$) limit. The explicit expression for this term can be found in ref 70. Another quantum-mechanical effect is introduced by the fact that the initial sampling of the positions and momenta is nonclassical. More specifically, the initial sampling of the positions is based on the exact quantum-mechanical position probability density, $\langle \mathbf{Q}_0|e^{-\beta H_b}|\mathbf{Q}_0\rangle/Z_b$, while the initial sampling of the momenta is based on the nonclassical probability density $\prod_{j=1}^{f}(1/\alpha^{(j)}\pi\hbar^2)^{1/2}\exp[-(P_{n,0}^{(j)})^2/\hbar^2\alpha^{(j)})]$.

III. Simulation Parameters and Techniques

The VER rate constant $k_{0\leftarrow 1}$ was calculated for H_2 and D_2 in liquid argon based on classical MD simulations and the LHA-LSC method. The temperature and density were chosen as $T = 152$ K and $\rho = 1.45\times 10^{22}$ cm^{-3}, respectively, in accord with the conditions for which experimental values of $k_{0\leftarrow 1}$ are available for both H_2 and D_2 in liquid argon.[4,19] The equilibrium bond length and vibrational frequencies for H_2 and D_2 were taken as 0.766640 Å,[84] 4400.4 cm^{-1},[83] and 3117.0 cm^{-1},[83] respectively. Thus, the values of $\beta\hbar\omega_0$ are 42 and 30 for H_2 and D_2, respectively. For comparison, the values of $\beta\hbar\omega_0$ in the previously studied heavier diatomic molecules N_2 and O_2 were 43 and 29, respectively (at 77 K). Thus, one expects a quantum enhancement of VER rates at least as strong as that observed for N_2 and O_2, and probably even stronger because of the significantly lighter mass of H_2 and D_2.

The classical MD simulations were initiated with 125 argon atoms arranged on a cubical lattice in a cubical simulation cell with standard periodic boundary conditions. One of the argon atoms was then replaced by a single H_2 or D_2 molecule. The system was then equilibrated at the desired temperature for 600 ps, using the velocity Verlet algorithm and Nose−Hoover chain thermostats of length four (one thermostat for each of the three

Cartesian coordinates of each argon atom and the diatomic molecule center of mass, and one for the three intramolecular DOF).[86] A time step of 1.0 fs was used in all the simulations reported in this paper, and the rigid molecule constraint was imposed via the Rattle algorithm.[87] The equilibration period was followed by a calculation of $C_{cl}(t)$, which involved averaging over 10^6 equilibrium trajectories, each of length 32.786 ps (2^{15} time steps). Once the FFCF was obtained, its FT was calculated via the FFT method. In the case of very high vibrational frequencies, the FT is a very small number and, therefore, very difficult to compute directly. Following common practice, we instead extrapolated the exponential gap law, which is observed to emerge at low frequencies, to higher frequencies.[88,89] Assuming that this extrapolation is the major source of error, we evaluated the error bars reported for the VER rate constants based on the least-squares fit to the corresponding linear frequency dependence of the VER rate constant on a semilog scale.

The calculation of the FFCF via the LHA-LSC method followed a procedure similar to that described in refs 69, 70, and 71. The main difference between the current and previous studies is that rather than restricting the LHA-LSC treatment to contributions from the first few solvation shells around the diatomic molecule, we were able to apply it to all of the atoms in the simulation cell (which was made possible by the availability of improved computer resources). The calculation starts by sampling the initial positions of all the atoms in the simulation cell via a path-integral MD (PIMD) simulation, where 16 beads were assigned to each atom. We have verified that assigning 32 beads per atom did not alter the results. The PIMD simulation was started with all 16 beads in the position of the corresponding atom in the above-mentioned cubical lattice configuration. This was followed by an equilibration period of 600 ps at the desired temperature, using the velocity Verlet algorithm and Nose−Hoover chain thermostats of length four (one thermostat for each of the three Cartesian coordinates of each argon atom bead and the diatomic molecule center of mass bead, and one for the three intramolecular DOF beads).[86] It should be noted that the initial configurations sampled satisfy the rigid molecule constraint.[70] The sampling was performed by choosing random beads from snapshots of the isomorphic liquid of cyclic polymers at each time step.

We would also like to note that treating the argon classically within the PIMD simulation did not alter the results significantly. This is consistent with the view that the force fluctuations are dominated by the motion of the much lighter H_2 and D_2 molecules. Nevertheless, all of the results reported here were based on PIMD simulations, where each argon atom was assigned 16 beads.

An overall number of 2×10^6 initial configurations were sampled via the above-mentioned PIMD-based procedure. For each of these, we calculated the normal-mode frequencies and transformation matrix via the Jacobi method[90] and used them in order to sample the initial normal mode momenta. Here, too, we restrict ourselves to normal-mode displacements that satisfy the constraints imposed by the rigidity of the H_2 and D_2 molecules.[70] It should also be noted that $\alpha^{(j)} > 0$ even if $\Omega^{(j)}$ is imaginary, as long as $\beta\hbar|\Omega^{(j)}| < \pi$. In fact, we did not find a single case where $\alpha^{(j)} < 0$ in over 120 000 initial configurations. Following the initial sampling, we performed a classical MD simulation over 2^{15} time steps for each of the initial configurations and extracted $C(t)$ from them. It should be noted that in calculating correlation functions via LHA-LSC, we can only correlate the forces at $t = 0$ and at a later time t. All of the results reported below were based on the cosine transform of the real part of the correlation functions.

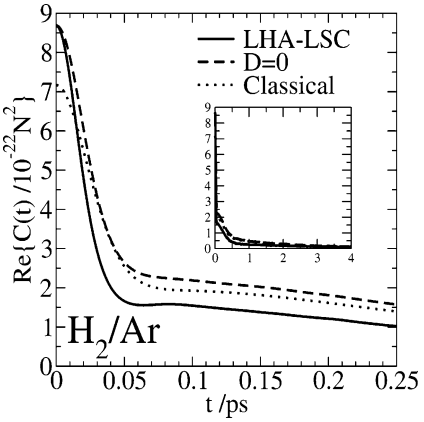

Figure 1. Real part of the force−force correlation function for H_2 in liquid argon at 152 K, as obtained via LHA-LSC (solid line), LHA-LSC with $D(\mathbf{Q}_0, \mathbf{P}_{n,0}) = 0$ (dashed line), and from classical MD simulations (dotted line). The decay of $C(t)$ at long times is shown in the insert.

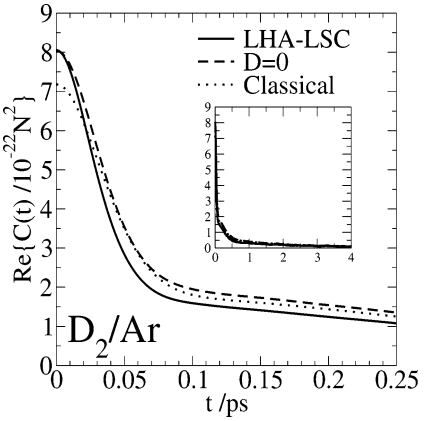

Figure 2. Real part of the force−force correlation function for D_2 in liquid argon at 152 K, as obtained via LHA-LSC (solid line), LHA-LSC with $D(\mathbf{Q}_0, \mathbf{P}_{n,0}) = 0$ (dashed line), and from classical MD simulations (dotted line). The decay of $C(t)$ at long times is shown in the insert.

IV. Results

The real parts of the FFCFs calculated for H_2−Ar and D_2−Ar via the LHA-LSC approximation are shown in Figures 1 and 2, respectively. Also shown in these figures are the results obtained by applying the LHA-LSC method with $D(\mathbf{Q}_0, \mathbf{P}_{n,0})$ set to zero (cf. eq 17), as well as the corresponding classical FFCFs. The FFCFs for both H_2−Ar and D_2−Ar are distinctly bimodal, with a rapid initial decay during the first ∼50 fs, followed by a significantly slower and long-lived decay that lasts for several picoseconds. This behavior is quite different in comparison to that of the FFCFs calculated for O_2 and N_2 in nonpolar solution. Clear deviations between the classical and semiclassical results are observed at short times (≤100 fs). Furthermore, the deviations in the case of H_2−Ar are larger than in the case of D_2−Ar, which is consistent with the expectation that quantum corrections should be more pronounced in the case of the lighter isotope. The most relevant difference between the classical and semiclassical results is that the LHA-LSC-based FFCF decays significantly faster than the classical FFCF. A more rapid decay translates into a larger high-frequency tail of the FFCF and, therefore, faster VER rates. The fact that neglecting the D term in the LHA-LSC ap-

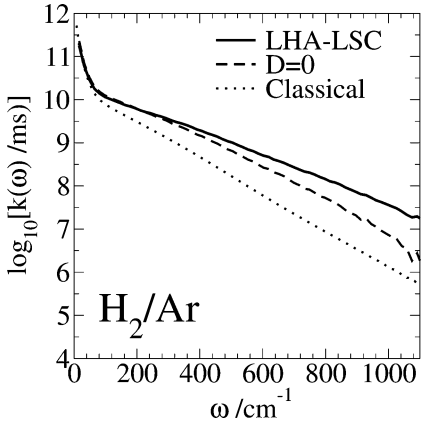

Figure 3. Frequency dependence of the VER rate constant, $k_{1\leftarrow 0}(\omega)$, for H_2 in liquid argon at 152 K, as obtained via LHA-LSC (solid line), LHA-LSC with $D(\mathbf{Q}_0, \mathbf{P}_{n,0}) = 0$ (dashed line), and from classical MD simulations (dotted line).

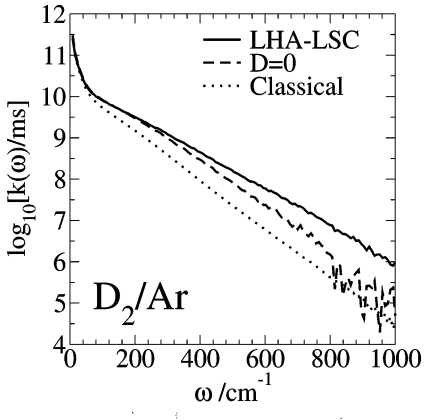

Figure 4. Frequency dependence of the VER rate constant, $k_{1\leftarrow 0}(\omega)$, for D_2 in liquid argon at 152 K, as obtained via LHA-LSC (solid line), LHA-LSC with $D(\mathbf{Q}_0, \mathbf{P}_{n,0}) = 0$ (dashed line), and from classical MD simulations (dotted line).

proximation yields a FFCF that decays more slowly demonstrates the importance of including this term in order to account for the full extent of the quantum enhancement.

The frequency-dependent VER rate constants, $k_{0\leftarrow 1}(\omega)$, for H_2-Ar and D_2-Ar are shown on a semilog plot in Figures 3 and 4, respectively. These results were obtained by calculating $\tilde{C}(\omega)$ from the real part of the FFCFs reported in Figures 1 and 2 (cf. eq 12) and substituting it into eq 11. As mentioned before, calculating the very small values of the FT of the FFCF at 4400.4 and 3117.0 cm^{-1} for H_2 and D_2, respectively, is not feasible. However, $k_{0\leftarrow 1}(\omega)$ is seen to follow an exponential gap law in the frequency range of $200-1000$ cm^{-1}. Following the commonly used procedure,[88,89] we assumed that the values of $k_{0\leftarrow 1}$ at higher frequencies can be calculated by extrapolating this exponential gap law. The VER rate constants that were obtained by following this procedure are reported in Table 1 alongside the corresponding experimental results.

The experimental VER rate constants for H_2-Ar and D_2-Ar are on the millisecond time scale, with the rate constant for H_2 an order of magnitude *larger* than that for D_2. The classical VER rate constants for the same systems are seen to be *slower* by $8-9$ orders of magnitude, with essentially the same values for H_2 and D_2. In comparison to this, the LHA-LSC-based VER rate constants are "only" $2-3$ orders of magnitude slower than experimental values. Also, the LHA-LSC-based VER rate constant for H_2 is an order of magnitude larger than that for D_2, similar to experiment. Neglecting the term $D(\mathbf{Q}_0, \mathbf{P}_{n,0})$ leads to VER rates that lie between the classical and full LHA-LSC results, but with the VER rate constant for H_2 still being an order of magnitude larger than that for D_2.

V. Discussion

The calculation of VER rates in H_2 and D_2 represents a considerable challenge because of the light masses *and* extremely high vibrational frequencies of these molecules, which can be expected to produce very pronounced quantum effects. Furthermore, one also expects a significant isotope effect in this system in light of the large mass ratio between H_2 and D_2. Indeed, the classical VER rates for H_2 and D_2 in liquid argon are found to be slower than the experimental VER rates by as much as $8-9$ orders of magnitude. In comparison, the classical VER rate constants of the heavier diatomic molecules O_2 and N_2 were found to be "only" 4 and 7 orders of magnitude slower than experiment, respectively. The experimental VER rate in H_2 is also found to be 1 order of magnitude faster than that in D_2 (despite the significantly larger vibrational frequency in the former).

In this paper, we have calculated the VER rate of H_2 and D_2 in liquid argon via the LHA-LSC method. It should be noted that this method was previously found to accurately predict VER rates in heavier high-frequency diatomic molecules, such as O_2 and N_2, under similar conditions.[70,71] While the agreement between the LHA-LSC-based and experimental VER rates is certainly not as good in the present case, it still represents a dramatic improvement in comparison to the corresponding classical predictions. Furthermore, unlike the classical results that show no significant isotope effect, the LHA-LSC-based results are consistent with the experimentally observed isotope effect.

In analyzing the isotope effect, it should be remembered that $k_{1\leftarrow 0}(H_2)/k_{1\leftarrow 0}(D_2) = \sqrt{\mu(D_2)/\mu(H_2)} \times \{\tilde{C}[\omega_0(H_2)]/\tilde{C}[\omega_0(D_2)]\}$. The term $\sqrt{\mu(D_2)/\mu(H_2)}$ enhances the VER rate of H_2 over that of D_2 by a factor of $\sqrt{2}$. The behavior of the term $\tilde{C}[\omega_0(H_2)]/\tilde{C}[\omega_0(D_2)]$ reflects the competition between two opposing driving forces. On the one hand, the fact that $\omega_0(H_2)/\omega_0(D_2) = \sqrt{2}$ implies that $\tilde{C}[\omega_0(H_2)]$ tends to be smaller than $\tilde{C}[\omega_0(D_2)]$ due to the lower density of accepting modes at higher frequencies. On the other hand, $\tilde{C}(\omega)$ follows a stronger exponential gap law for D_2 than for H_2. This implies that, for a given frequency, H_2 has more accepting modes than D_2. Classically, this can be traced back to the lower reduced mass of H_2, which implies that momentum exchange with the solvent atoms would be more efficient. This explains why the classical VER rates for H_2 and D_2 are almost identical despite the fact that $\omega(H_2)$ is significantly larger than $\omega(D_2)$. However, the classical treatment does not account for the order of magnitude difference between the VER rates of H_2 and D_2. In contrast, the LHA-LSC method captures this difference, which suggests that its origin is purely quantum-mechanical. More specifically, the smaller mass of H_2 implies that it can more deeply penetrate classically forbidden regions of the repulsive part of the interaction potential, thereby sampling stronger forces that lead to enhancement of its VER rate.

It should be noted that, although the LHA-LSC method accurately captures the isotope effect and provides VER rates that are in far better agreement with experiment than the corresponding classical predictions, they are still about $2-3$ orders of magnitude slower in comparison to the experimental

TABLE 1: VER Rate Constants for H_2 and D_2 and Their Ratio in Liquid Argon at $T = 152$ K and $\rho = 1.45 \times 10^{22}$ cm^{-3}[a]

	$k_{0\leftarrow1}(H_2)$/ms^{-1}	$k_{0\leftarrow1}(D_2)$/ms^{-1}	$k_{0\leftarrow1}(H_2)/k_{0\leftarrow1}1(D_2)$
experiment	4.46 (ref 4)	0.32 (ref 19)	14
classical	$(1.9 \pm 0.2) \times 10^{-9}$	$(2.5 \pm 0.3) \times 10^{-9}$	0.8 ± 0.2
LHA-LSC ($D = 0$)	$(1.7 \pm 0.7) \times 10^{-5}$	$(1.2 \pm 0.3) \times 10^{-6}$	14 ± 7
LHA-LSC	$(1.0 \pm 0.2) \times 10^{-2}$	$(4.9 \pm 0.7) \times 10^{-4}$	20 ± 5
QCF	$(4.2 \pm 0.4) \times 10^{-4}$	$(2.2 \pm 0.3) \times 10^{-5}$	19 ± 4

[a] The experimental result reported for H_2 corresponds to the average of the experimental results obtained for $\rho = 1.40 \times 10^{22}$ cm^{-3} and $\rho = 1.53 \times 10^{22}$ cm^{-3} at 150 K. Also shown are the classical results, the results obtained via the LHA-LSC method with and without the term $D(\mathbf{Q_0}, \mathbf{P_{n,0}})$, and the results obtained by using the mixed Harmonic−Schofield QCF.[57]

VER rates. Several reasons may contribute to this discrepancy. First, it is possible that the force fields used are not accurate enough, particularly in the repulsive region. However, this seems unlikely in light of the high quality of the H_2−Ar and D_2−Ar interaction potentials used. Another possibility is that the experimental VER rates involved contributions from processes that are not accounted for in our model. For example, the experimental procedure of extrapolating from finite to infinite dilution may be inaccurate. Yet another possibility is that the discrepancy arises from assuming that the exponential gap law obtained at low frequencies ($\leq$1000 cm^{-1}) can be extrapolated to much higher frequencies. For example, we have found that using the alternative extrapolation procedure proposed in ref 42 yields VER rates that are in better agreement with experiment ($\sim$0.7 ms^{-1} and 1.4×10^{-2} ms^{-1} for H_2−Ar and D_2−Ar respectively). This procedure is based on fitting the FFCF at short times to an ansatz whose FT is known analytically. We have found that the two procedures lead to results that can be fitted to essentially the same exponential gap law at low frequencies. However, this ansatz-based approach also predicts that the slope of the exponential gap law slowly *decreases* with increasing frequency, which leads to the prediction of somewhat faster VER rates. However, it should be noted that the choice of ansatz is motivated by mathematical convenience rather than by the underlying physics. Thus, the decreasing slope of the exponential gap law may well be an artifact that results from the choice of ansatz. Nevertheless, this result suggests that extrapolating the low-frequency exponential gap law from low to high frequencies may not be entirely accurate. A direct calculation of the VER rate constant at high frequencies would obviously be highly desirable. Unfortunately, such a direct calculation is not feasible at the present time.

Finally, one should also consider the possibility that the discrepancy between the LHA-LSC-based and experimental VER rates is due to the approximations underlying the LHA-LSC method. In this context, it is interesting to note that a much better agreement between the LHA-LSC-based and experimental VER rates was observed for O_2 and N_2, despite the fact that the corresponding values of $\beta\hbar\omega_0$ were essentially the same as those considered here for H_2 and D_2.[70,71] It should also be noted that the quantum enhancement of VER rates in H_2 and D_2 is several orders of magnitude larger than that in O_2 and N_2. A similar trend is also observed when one attempts to estimate the quantum-mechanical VER rates in H_2 and D_2 via the QCF approach. More specifically, it has been argued by Skinner and co-workers that the mixed harmonic−Schofield QCF should be used in the case of VER of a high-frequency homonuclear diatomic molecule in a nonpolar solvent.[57] Indeed, comparison between different QCFs showed that using this QCF led to the best agreement with experiment in the case of O_2 and N_2.[71] Furthermore, the VER rates obtained by using this QCF were found to be similar to these obtained via the LHA-LSC method.[71] However, when applied to H_2 and D_2, this QCF predicts VER rate constants that are about 4 orders of magnitude slower than the experimental ones (cf. Table 1). Nonetheless, the ratio of the QCF-based VER rate constants for H_2 and D_2 is in good agreement with experiment. These observations give rise to the intriguing possibility that the VER of H_2 and D_2 is sensitive to quantum effects that cannot be captured by either the LHA-LSC method or the QCF approach. Furthermore, because these effects seem to be sensitive to the mass of the diatomic molecule and because both the LHA-LSC and QCF approaches rely on purely classical dynamics, one may speculate that the missing quantum affects are of a dynamical nature. Further insight into this issue can be gained by calculating the VER rates for H_2 and D_2 via other, possibly more accurate, methods such as the semiclassical initial-value-representation method,[91,92] quantum mode-coupling theory,[93] and the analytical continuation approach.[94−99]

Acknowledgment. This project was supported by the National Science Foundation through grant no. CHE-0306695. The authors would also like to thank Dr. Being J. Ka and Dr. Qiang Shi for helpful discussions and advice.

Appendix A: Explicit Expressions for $U(0)$ and F

The potential energy of the bath is given by (cf. eq 9):

$$U(q=0) = \sum_{j=1}^{N} \sum_{j<k} \phi_{\mathrm{Ar-Ar}}(r_{jk}) + \sum_{j=1}^{N} \phi_{\mathrm{H_2-Ar}}(r_{j0},\theta_j,q=0) \tag{A1}$$

Here, $\phi_{\mathrm{H_2-Ar}}(R,\theta,q=0) = V_{\mathrm{HL}}(R,\theta,q=0) + V_{\mathrm{C}}(R,\theta,q=0)$ (cf. eq 8), where

$$V_{\mathrm{HL}}(R,\theta,q=0) = K[F_{0,0} + F_{2,0}P_2(\cos\theta)] \exp\{-(R - R_s(\theta))[b_0 + b_1 z(\theta) + b_2 z^2(\theta)]\} \sum_{\lambda=0(2)}^{6} \sum_{p=0}^{3} a_{p0}^{\lambda} z^p(\theta) P_\lambda(\cos\theta) \tag{A2}$$

and

$$V_{\mathrm{C}}(R,\theta,q=0) = -G_{10}(R,\theta) \sum_{n=6(2)}^{10} \sum_{\lambda=0(2)}^{n-4} f_n(R,\theta) R^{-n} C_n{}^{\lambda}0 P_\lambda (\cos\theta) \tag{A3}$$

The functions and parameters in eqs A2 and A3 are defined as in ref 84.

The force exerted on the vibrational mode by the bath is given by (cf. eq 9):

$$F = -\left.\frac{\partial U(q)}{\partial q}\right|_{q=0} = -\sum_{j=1}^{N} \left.\frac{\partial}{\partial q} \phi_{\mathrm{H_2-Ar}}(r_{j0},\theta_j,q)\right|_{q=0} \tag{A4}$$

Here $\partial\phi_{H_2-Ar}(R,\theta,q)\partial q|_{q=0} = \partial V_{HL}(R,\theta,q)\partial q|_{q=0} + \partial V_C(R,\theta,q)\partial q|_{q=0}$ (cf. eq 8), where

$$\left.\frac{\partial V_{HL}}{\partial q}\right|_{q=0} = \frac{1}{r_0}K \exp\{-(R - R_s(\theta))[b_0 + b_1 z(\theta) + b_2 z^2(q)]\} \sum_{\lambda=0(2)}^{6} \sum_{p=0}^{3} z^p(\theta) P_\lambda(\cos\theta)[(F_{0,0} + F_{2,0}P_2(\cos\theta))a_{p1}^{\lambda} + (F_{0,1} + F_{2,1}P_2(\cos\theta))a_{p0}^{\lambda}] \quad \text{(A5)}$$

and

$$\left.\frac{\partial V_C}{\partial q}\right|_{q=0} = -\frac{1}{r_0}G_{10}(R,\theta) \sum_{n=6(2)}^{10} \sum_{\lambda=0(2)}^{n-4} f_n(R,\theta)R^{-n}C_n^{\lambda}1P_\lambda (\cos\theta) \quad \text{(A6)}$$

The functions and parameters in eqs A5 and A6 are defined as in ref 84.

References and Notes

(1) Brueck, S. R. J.; Osgood, R. M. *Chem. Phys. Lett.* **1976** *39*, 568.
(2) Chateau, M.; Delalande, C.; Frey, R.; Gale, G. M.; Pradère, F. *J. Chem. Phys.* **1979**, *71*, 4799.
(3) Delalande, C.; Gale, G. M. *J. Chem. Phys.* **1979**, *71*, 4804.
(4) Delalande, C.; Gale, G. M. *J. Chem. Phys.* **1980**, *73*, 1918.
(5) Faltermeier, B.; Protz, R.; Maier, M.; Werner, E. *Chem. Phys. Lett.* **1980**, *74*, 425.
(6) Faltermeier, B.; Protz, R.; Maier, M. *Chem. Phys.* **1981**, *62*, 377 .
(7) Oxtoby, D. W. *Adv. Chem. Phys.* **1981**, *47* (Part 2), 487.
(8) Oxtoby, D. W. *Annu. Rev. Phys. Chem.* **1981**, *32*, 77.
(9) Oxtoby, D. W. *J. Phys. Chem.* **1983**, *87*, 3028.
(10) Chesnoy, J.; Gale, G. M. *Ann. Phys. Fr.* **1984**, *9*, 893.
(11) Chesnoy, J.; Gale, G. M. *Adv. Chem. Phys.* **1988**, *70* (Part 2), 297.
(12) Harris, C. B.; Smith, D. E.; Russell, D. J. *Chem. Rev.* **1990**, *90*, 481.
(13) Miller, D. W.; Adelman, S. A. *Int. Rev. Phys. Chem.* **1994**, *13*, 359.
(14) Stratt, R. M.; Maroncelli, M. *J. Phys. Chem.* **1996**, *100*, 12981.
(15) Owrutsky, J. C.; Raftery, D.; Hochstrasser, R. M. *Annu. Rev. Phys. Chem.* **1994**, *45*, 519.
(16) Elsaesser, T.; Kaiser, W. *Annu. Rev. Phys. Chem.* **1991**, *42*, 83.
(17) Calaway, W. F.; Ewing, G. E. *J. Chem. Phys.* **1975**, *63*, 2842.
(18) Laubereau, A.; Kaiser, W. *Rev. Mod. Phys.* **1978**, *50*, 607.
(19) Roussignol, P.; Delalande, C.; Gale, G. M. *Chem. Phys.* **1982**, *70*, 319.
(20) Heilweil, E. J.; Doany, F. E.; Moore, R.; Hochstrasser, R. M. *J. Chem. Phys.* **1982**, *76*, 5632.
(21) Heilweil, E. J.; Casassa, M. P.; Cavanagh, R. R.; Stephenson, J. C. *Chem. Phys. Lett.* **1985**, *117*, 185.
(22) Heilweil, E. J.; Casassa, M. P.; Cavanagh, R. R.; Stephenson, J. C. *J. Chem. Phys.* **1986**, *85*, 5004.
(23) Harris, A. L.; Brown, J. K.; Harris, C. B. *Annu. Rev. Phys. Chem.* **1988**, *39*, 341.
(24) Paige, M. E.; Russell, D. J.; Harris, C. B. *J. Chem. Phys.* **1986**, *85*, 3699.
(25) Owrutsky, J. C.; Kim, Y. R.; Li, M.; Sarisky, M. J.; Hochstrasser, R. M. *Chem. Phys. Lett.* **1991**, *184*, 368.
(26) Moustakas, A.; Weitz, E. *J. Chem. Phys.* **1993**, *98*, 6947.
(27) Kliner, D. A. V.; Alfano, J. C.; Barbara, P. F. *J. Chem. Phys.* **1993**, *98*, 5375.
(28) Zimdars, D.; Tokmakoff, A.; Chen, S.; Greenfield, S. R.; Fayer, M. D.; Smith, T. I.; Schwettman, H. A. *Phys. Rev. Lett.* **1993**, *70*, 2718.
(29) Pugliano, N.; Szarka, A. Z.; Gnanakaran, S.; Hochstrasser, R. M. *J. Chem. Phys.* **1995**, *103*, 6498.
(30) Paige, M. E.; Harris, C. B. *Chem. Phys.* **1990**, *149*, 37.
(31) Salloum, A.; Dubost, H. *Chem. Phys.* **1994**, *189*, 179.
(32) Tokmakoff, A.; Sauter, B.; Fayer, M. D. *J. Chem. Phys.* **1994**, *100*, 9035.
(33) Tokmakoff, A.; Fayer, M. D. *J. Chem. Phys.* **1995**, *103*, 2810.
(34) Urdahl, R. S.; Myers, D. J.; Rector, K. D.; Davis, P. H.; Cherayil, B. J.; Fayer, M. D. *J. Chem. Phys.* **1997**, *107*, 3747.
(35) Owrutsky, J. C.; Li, M.; Locke, B.; Hochstrasser, R. M. *J. Phys. Chem.* **1995**, *99*, 4842.
(36) Laenen, R.; Rauscher, C.; Laubereau, A. *Phys. Rev. Lett.* **1998**, *80*, 2622.
(37) Woutersen, S.; Emmerichs, U.; Nienhuys, H.; Bakker, H. J. *Phys. Rev. Lett.* **1998**, *81*, 1106.
(38) Myers, D. J.; Urdahl, R. S.; Cherayil, B. J.; Fayer, M. D. *J. Chem. Phys.* **1997**, *107*, 9741.
(39) Myers, D. J.; Chen, S.; Shigeiwa, M.; Cherayil, B. J.; Fayer, M. D. *J. Chem. Phys.* **1998**, *109*, 5971.
(40) Sagnella, D. E.; Straub, J. E.; Jackson, T. A.; Lim, M.; Anfinrud, P. A. *Proc. Natl. Acad. Sci. U.S.A.* **1999**, *96*, 14324.
(41) Hamm, P.; Lim, M.; Hochstrasser, R. M. *J. Chem. Phys.* **1997**, *107*, 1523.
(42) Egorov, S. A.; Skinner, J. L. *J. Chem. Phys.* **1996**, *105*, 7047.
(43) Everitt, K. F.; Egorov, S. A.; Skinner, J. L. *Chem. Phys.* **1998**, *235*, 115.
(44) Everitt, K. F.; Skinner, J. L. *J. Chem. Phys.* **1999**, *110*, 4467.
(45) Lawrence, C. P.; Skinner, J. L. *J. Chem. Phys.* **2002**, *117*, 5827.
(46) Deng, Y.; Stratt, R. M. *J. Chem. Phys.* **2002**, *117*, 1735.
(47) Deng, Y.; Stratt, R. M. *J. Chem. Phys.* **2002**, *117*, 10752.
(48) Sibert, E. L., III; Rey, R. *J. Chem. Phys.* **2002**, *116*, 237.
(49) Li, S.; Thompson, W. H. *J. Chem. Phys.* **2003**, *107*, 8696.
(50) Zwanzig, R. *J. Chem. Phys.* **1961**, *34*, 1931.
(51) Landau, L.; Teller, E. Z. *Z. Sowjetunion* **1936**, *34*, 10.
(52) Makri, N. *Annu. Rev. Phys. Chem.* **1999**, *50*, 167.
(53) Berne, B. J.; Jortner, J.; Gordon, R. *J. Chem. Phys.* **1967**, *47*, 1600.
(54) Bader, J. S.; Berne, B. J. *J. Chem. Phys.* **1994**, *100*, 8359.
(55) Egorov, S. A.; Everitt, K. F.; Skinner, J. L. *J. Phys. Chem. A* **1999**, *103*, 9494.
(56) Egorov, S. A.; Skinner, J. L. *J. Chem. Phys.* **2000**, *112*, 275.
(57) Skinner, J. L.; Park, K. *J. Phys. Chem. B* **2001**, *105*, 6716.
(58) Rostkier-Edelstein, D.; Graf, P.; Nitzan, A. *J. Chem. Phys.* **1997**, *107*, 10470.
(59) Rostkier-Edelstein, D.; Graf, P.; Nitzan, A. *J. Chem. Phys.* **1998**, *108*, 9598.
(60) Everitt, K. F.; Skinner, J. L.; Ladanyi, B. M. *J. Chem. Phys.* **2002**, *116*, 179.
(61) Berens, P. H.; White, S. R.; Wilson, K. R. *J. Chem. Phys.* **1981**, *75*, 515.
(62) Frommhold, L. *Collision-Induced Absorption in Gases*; *Cambridge Monographs on Atomic, Molecular, and Chemical Physics*, 1st ed.; Cambridge University Press: Cambridge, 1993; Vol. 2.
(63) Skinner, J. L. *J. Chem. Phys.* **1997**, *107*, 8717.
(64) An, S. C.; Montrose, C. J.; Litovitz, T. A. *J. Chem. Phys.* **1976**, *64*, 3717.
(65) Egorov, S. A.; Skinner, J. L. *Chem. Phys. Lett.* **1998**, *293*, 439.
(66) Schofield, P. *Phys. Rev. Lett.* **1960**, *4*, 239.
(67) Egelstaff, P. A. *Adv. Phys.* **1962**, *11*, 203.
(68) Kneller, G. R. *Mol. Phys.* **1994**, *83*, 63.
(69) Shi, Q.; Geva, E. *J. Phys. Chem. A* **2003**, *107*, 9059.
(70) Shi, Q.; Geva, E. *J. Phys. Chem. A* **2003**, *107*, 9070.
(71) Ka, B. J.; Shi, Q.; Geva, E. *J. Phys. Chem. A* **2005**, *109*, 5527.
(72) Ka, B. J.; Geva, E. *J. Phys. Chem. A* **2006**, *110*, 9555.
(73) Shi, Q.; Geva, E. *J. Chem. Phys.* **2003**, *118*, 8173.
(74) Sun, X.; Miller, W. H. *J. Chem. Phys.* **1997**, *106*, 916.
(75) Wang, H.; Sun, X.; Miller, W. H. *J. Chem. Phys.* **1998**, *108*, 9726.
(76) Sun, X.; Wang, H.; Miller, W. H. *J. Chem. Phys.* **1998**, *109*, 4190.
(77) Sun, X.; Wang, H.; Miller, W. H. *J. Chem. Phys.* **1998**, *109*, 7064.
(78) Wang, H.; Song, X.; Chandler, D.; Miller, W. H. *J. Chem. Phys.* **1999**, *110*, 4828.
(79) Sun, X.; Miller, W. H. *J. Chem. Phys.* **1999**, *110*, 6635.
(80) Wang, H.; Thoss, M.; Miller, W. H. *J. Chem. Phys.* **2000**, *112*, 47.
(81) Shemetulskis, N. E.; Loring, R. F. *J. Chem. Phys.* **1992**, *97*, 1217.
(82) Hillery, M.; O'Connell, R. F.; Scully, M. O.; Wigner, E. P. *Phys. Rep.* **1984**, *106*, 121.
(83) Miller, D. W.; Adelman, S. A. *J. Chem. Phys.* **2002**, *117*, 2688.
(84) Bissonnette, C.; Chuaqui, C. E.; Crowell, K. G.; Le Roy, R. J.; Wheatley, R. J.; Meath, W. J. *J. Chem. Phys.* **1996**, *105*, 2639.
(85) Jang, J.; Stratt, R. M. *J. Chem. Phys.* **2000**, *113*, 5901.
(86) Jang, S.; Voth, G. A. *J. Chem. Phys.* **1997**, *107*, 9514.
(87) Andersen, H. C. *J. Comput. Phys.* **1983**, *52*, 24.
(88) Nitzan, A.; Mukamel, S.; Jortner, J. *J. Chem. Phys.* **1974**, *60*, 3929.
(89) Nitzan, A.; Mukamel, S.; Jortner, J. *J. Chem. Phys.* **1975**, *63*, 200.
(90) Press, W. H.; Flannery, B. P.; Teukolsky, S. A.; Vetterling, W. T. *Numerical Recipes*; Cambridge University Press: Cambridge, 1986.
(91) Miller, W. H. *J. Phys. Chem. A* **2001**, *105*, 2942.
(92) Makri, N.; Miller, W. H. *J. Chem. Phys.* **2002**, *116*, 9207.

(93) Reichman, D. R.; Rabani, E. *Annu. Rev. Phys. Chem*. **2005**, *56*, 157.
(94) Gallicchio, E.; Berne, B. J. *J. Chem. Phys.* **1996**, *105*, 7064.
(95) Gallicchio, E.; Egorov, S. A.; Berne, B. J. *J. Chem. Phys.* **1998**, *109*, 7745.
(96) Egorov, S. A.; Gallicchio, E.; Berne, B. J. *J. Chem. Phys.* **1997**, *107*, 9312.
(97) Rabani, E.; Krilov, G.; Berne, B. J. *J. Chem. Phys.* **2000**, *112*, 2605.
(98) Rabani, E.; Reichman, D. R.; Krylov, G.; Berne, B. J. *Proc. Natl. Acad. Sci. U.S.A.* **2002**, *99*, 1129.
(99) Golosov, A. A.; Reichman, D. R.; Rabani, E. *J. Chem. Phys.* **2003**, *118*, 457.